Supplementary Methods

Design and Construction of Computationally Directed Library. The pmut_scan protocol in the Rosetta molecular modeling suite was used to evaluate all possible point mutations in AsLOV2 (PDB: 2v0u). The set of all possible point mutations was filtered to include only mutations that decreased the Rosetta score or increased it by less than 1 REU (Rosetta Energy Unit). For a few positions on the PAS β sheet mutations with ΔΔG's of +2 REU's were allowed. The list was then filtered to only include mutations that were within 6Å of the Jα helix. The resulting library contained 743 mutations at 49 positions (additional mutations were allowed due to degenerate primer design). The Rosetta-biased point-mutant library was constructed using a comprehensive mutagenesis protocol (1). Mutagenic oligos with degenerate codons flanked by 15-18 bases were pooled. 200 picomoles of the oligo pool were incubated with 20 units of T4 Polynucleotide kinase (NEB) for 1 hour at 37˚C in the presence of 1x T4 PNK buffer. The enzyme was heat-inactivated at 65˚C for 20 minutes. Single-stranded template uracil-DNA encoding TorA-LovSsrA-pIII_C-terminal domain was amplified and purified as described (2). One microgram of template DNA (0.75 picomoles) were combined with 2-fold excess 5'-phosphorylated oligo pool. Template-oligo annealing followed by polymerase extension and ligation of the mutagenic strand was performed as described (1). Template DNA was degraded with 5 units of Uracil DNA Glycosylase (NEB) and 2 units of Exonuclease III (NEB) before desalting and electroporation into SS320 cells. The experimental library size was 5×10^7, which most likely samples all possible point-mutants and a large fraction of double-mutants.

Construction of the shuffled library. Mutagenic oligos encoding substitutions suggested by the primary ELISA screens of the point-mutant library were pooled and assembled using a gene-assembly protocol. Gene-SOE PCR was performed with Q5 DNA Polymerase (NEB), 1 μM total oligo (31 total oligos) and the following cycling conditions: 20 cycles of (98˚C 10s, 52˚C 30s, 72˚C 10s) in 50 μL. One μL of the assembled product was PCR-amplified using outside primers for restriction cloning. Two μg's of linearized and gel purified pFNOM6-tat-pIII plasmid was ligated to 1 μg of shuffled-lovssrA library insert (4:1 insert:vector ratio). Ligated DNA was ethanol precipitated and electroporated into SS320 cells. The number of total transformants was 2×10^8, which partially covers the designed sequence space (1.2×10^8).

Phage Display Selection Against SspB. The LOV library was expressed as an N-terminal fusion of the phage pIII coat protein using the tat secretion pathway as export via the DsbA signal peptide pathway was not possible (Fig. S10). All libraries were subjected to four rounds of panning prior to ELISA screening. Maxisorp 96-well plates were coated overnight at 4˚C with 100 μg/mL of 5 micrograms/mL His-MBP-SspB fusion in the presence of 50 mM sodium bicarbonate pH 9.6 buffer. Coated wells were washed with PBS-0.1% (v/v) Tween (PBST) and blocked at room temperature for 2 hours with 200 μL of PBST-BSA (5 mg/mL). Blocked wells are washed with PBST and incubated with 10^{11} – 10^{12} library phages for 1 hour under a

collimated blue LED array (1.2 mW*cm^{-2} at 450nm). Wells were washed 10-times with PBST while keeping the plate under blue light. Plates were moved into dark and incubated in the dark for 10 minutes. Dissociating phages were collected with PBST buffer. Early log SS320 cells (OD_{600}: 0.2-0.5) were infected with eluted phage and infected cells were grown in 25 mL 2xTY media supplemented with 100 µg/mL of ampicillin. When cells reach early log phase, M13KO7 helper phage was added with 20:1 multiplicity of infection. Following a 20-minute incubation at 37˚C without shaking, 0.1 mM IPTG and 5 µM flavin mononucleotide (FMN) were added and the culture was moved to a 30˚C shaker covered with foil to ensure dark conditions. After 1.5 hour, kanamycin was added to 25 µg/mL and the culture was grown overnight. The following day, the phage was PEG-precipitated and quantified using A_{268} values (2). Gene pool post-Round-4 selection was PCR amplified and cloned into a previously modified pET21b vector that introduces an N-terminal FLAG epitope. The ligation reaction was directly transformed into BL21(DE3)pLysS cells for protein expression and ELISA screening.

Fasta of Tat-oLID-p3
>MNNNDLFQASRRRFLAQLGGLTVAGMLGPSLLTPRRATAGSGEFLATTLERIEKNFVIT
DPRLPDNPIIFASDSFLQLTEYSREEILGRNCRFLQGPETDRATVRKIRDAIDNQTEVTVQ
LINYTKSGKKFWNLFHLQPMRDQKGDVQYFIGVQLDGTEHVRDAAEREAVMLIKKTAEEI
DEAANDENYFSGLESRGPFSGDFDYEKMANANKGAMTENADENALQSDAKGKLDSVAT
DYGAAIDGFIGDVSGLANGNGATGDFAGSNSQMAQVGDGDNSPLMNNFRQYLPSLPQSVE
CRPFVFSAGKPYEFSIDCDKINLFRGVFAFLLYVATFMYVFSTFANILRNKES
Fasta of DsbA-oLID-p3
>MKKIWLALAGLVLAFSASAAELAAAGSGEFLATTLERIEKNFVITDPRLPDNPIIFASDSF
LQLTEYSREEILGRNCRFLQGPETDRATVRKIRDAIDNQTEVTVQLINYTKSGKKFWNLFH
LQPMRDQKGDVQYFIGVQLDGTEHVRDAAEREAVMLIKKTAEEIDEAANDENYFLESRGP
FEGKPIPNPLLGLDSTRPFVCEYQGQSSDLPQPPVNAGGGSGGGSGGGSEGGGSEGGGSEG
GGSEGGGSGGGSGSGDFDYEKMANANKGAMTENADENALQSDAKGKLDSVATDYGAAID
GFIGDVSGLANGNGATGDFAGSNSQMAQVGDGDNSPLMNNFRQYLPSLPQSVECRPFVFS
AGKPYEFSIDCDKINLFRGVFAFLLYVATFMYVFSTFANILRNKES

Photoswitch Evaluation by Soluble Protein ELISA. BL21(DE3)pLysS cells carrying pET21b_FLAG_LovssrA clones were plated on LB/Amp plates. Next day, 96-well growth blocks containing 500 µL LB medium supplemented with 25 µg/mL chloramphenicol, 100 µg/mL ampicillin, and 0.6 mM IPTG were inoculated with individual colonies and grown overnight in the dark at 30˚C. One well per plate was reserved for the parent for comparison. 200 µl of cells were lysed in the dark with 10 µl Popculture reagent and 1 unit of Benzonase nuclease for 15 minutes. Lysates were centrifuged and supernatant diluted 5-10 fold in PBST with 1mM DTT was used for the assays. Duplicate Maxisorp plates (96-well or 384-well) were coated with His-MBP-SspB as described above. Plates were blocked with PBS-3% (m/v) BSA and incubated with the lysate supernatant for 1 hour in the dark and under blue-light (1.2 mW*cm^{-2} at 450nm, collimated blue LED array). Plates were washed 5 times with PBST and incubated for 30 minutes with 1:20,000 diluted anti-FLAG antibody HRP conjugate (Sigma A8592). Plates were washed 3 times with PBST and

twice with PBS. 100 µl TMB was added and color was developed for 15 minutes. The reaction was quenched with 100 µl 0.5 M sulfuric acid before measuring A_{450}. LovssrA variants for the positive clones were PCR amplified using 4 µl cells as template and sequenced.

Growth and Purification of Recombinant Proteins. All expressed and purified proteins were cloned into the pQE-80L protein expression vector. All LOV clones contained an N-terminal 6x(His) tag and SspB clones contained an N-terminal 6x(His)-MBP-TEV site tag. Sequence-verified clones were transformed into BL21(DE3)pLysS *E.Coli* cells. Cultures were grown to an OD of 0.6 at 37°C, then induced with 333 mM IPTG and moved to 18°C for 16 hours. Cell pellets were resuspended in loading buffer (50 mM sodium phosphate pH 7.5, 500 mM NaCl, 20 mM Imidazole, 100 µM PMSF). Resuspended cells were sonicated and lysate spun down for 30 minutes at 20,000 rpm. Proteins of interest were isolated via Ni^{2+} affinity chromatography using HisTrap HP columns (GE), and eluted with elution buffer (50mM phosphate pH 7.5, 500 mM NaCl, and 500 mM imidazole). Proteins expressed as MBP fusions were then cut with TEV, dialyzed overnight into loading buffer, and re-run over the HisTrap HP column, collecting the tag-less protein. Finally, size exclusion chromatography with a Superdex 75 column (GE) was used for a final cleanup step and buffer exchange to final binding buffer, PBS (10 mM dibasic sodium phosphate, 1.8 mM monobasic potassium phosphate, 137 mM NaCl, 2.7 mM KCl). Protein concentration was determined via BCA protein assay (Pierce). Expression (*E.coli* & mammalian) constructs of iLID and SspB variants used can be found in Table S6 and will be available on Addgene.

Fluorescence Polarization Binding Assays. Fluorescence polarization experiments were conducted with a Jobin Yvon Horiba FluoroMax3 spectrofluorometer in a 1 cm quartz cuvette. Polarization of the TAMARA-SsrA peptide was measured through excitation at 555 nm and emission at 584 nm. For direct binding experiments between SspB and TAMARA-SsrA, starting peptide concentration was 25 nM in PBS. For competitive binding assays, 25 nM TAMARA-SsrA and 40 nM SspB (in PBS) were incubated prior to titrating LOV fusions. At each titration, the sample was irradiated with 6.0 $mW*cm^{-2}$ blue light for 1 minute, turned off and a lit state polarization was measured. After 5 minutes in the dark, a second measurement was taken, representing the dark state population.

Thermal Reversion Assay. Purified iLID protein was dialyzed against 4L of PBS buffer twice before measuring reversion kinetics. Protein samples were prepared at 10µM and allowed to equilibrate to room temperature in a 1cm quartz cuvette. Samples were then irradiated with blue light (6.0 $mW*cm^{-2}$ at 450nm, collimated blue LED array) for 30 seconds. Recovery of absorbance at 450nm was then measured every 0.1 seconds for 5 minutes.

Crystallization and Structural Determination of iLid. Initial crystals of iLid were grown using hanging drop vapor diffusion. Drops consisted of 2 µL well solution (800 mM lithium chloride, 100 mM TRIS:HCl pH 8.5, 32% (m/v) PEG 4000) and 1 µL

iLid protein (10 mg/mL in 100mM ammonium acetate). Initial conditions were optimized by microseeding. Final crystal drops were 2 µL well solution, 1 µL iLid (10 mg/mL), 0.5 µL microseed solution. Crystals grew to maximum size in 3 days. X-ray diffraction data was collected at Southeast Regional Collaborative Access Team (SER-CAT) 22-ID beamline at the Advanced Photon Source, Argonne National Laboratory. Data was indexed with XDS and scaled with Scala (3–5). The structure of iLid was determined using PAS fold residues N414-D515 of PDB id 2v0u as a molecular replacement model in Phaser (6). Phenix and Coot were used to iteratively refine the final structure (7, 8).

Mammalian Cell Localization/GEF Microscopy and Image Analysis. IA32 mouse fibroblasts were transfected in 6 well tissue culture plates with equal amounts of 2 vectors, each containing a component of the switch (ex. 0.5 µg pll7.0 Venus-iLID-CAAX : 0.5 µg pll7.0 tgRFPt –Nano; See Table S6 for vector information). 24 hr after transfection and 24 hr before image aquisition, cells were plated on No. 0 glass bottomed dishes (MatTek) coated with a 10 µg/ml solution of Fibronectin. Image acquisition was performed using a FluoView FV1000 scanning confocal inverted microscope equipped with a 1.30 N.A. 40 x oil immersion objective, a Hamamatsu PMT, environmental chamber (Precision Plastics) and controlled by Fluoview software (Olympus, Version 3.1b). A 25 mW argon laser provided the 488 nm and 515 nm laser lines while a 15 mW diode laser provided the 559 nm laser line. The environmental chamber was used to continue culture at 37° C and 5 (v/v) CO_2 throughout image acquisition. The software Time Controller was used to set a timeline of image acquisition and LOV domain excitation within a predefined region of interest. During periods of excitation, the ROIs were continuously scanned with 488 nm light except during the time it took to aquire an image (< 3 sec). 1% power of the 488 nm laser was used for all LOV domain excitation. During all experiments, images were acquired every 10 sec before and after excitation while image acquisition times varied during each type of excitation, due to the difference in excitation area. For spot activation and whole cell activation LOV excitation and image acquisition required 7.6 sec 14.7 sec respectively.
All images were analyzed using FIJI software (9). For spot activation, the average tgRFPt fluorescence intensity within the activated ROI was measured for each frame and the background subtracted. The values for each image set were normalized to the average of the first three frames before excitation. For half-cell activation, ROIs of similar tgRFPt fluorescence were manually chosen within the activated area and outside the activated area. Mean values were acquired for each frame and background subtracted. The reported values are a ratio of the fluorescence inside to outside the activated area. For whole cell activation, analysis was automated. For each frame, ROIs were produced by applying the default Auto Threshold function to the Venus channel(Mito ROI). To produce a Cyto ROI the Mito ROI was expanded by 10 pixels and then removed from the new ROI. The average tgRFPt intensity was then measured for each ROI and frame. The ratio of mitochondrial to cytoplasmic signal was then calculated for each frame like so: (Mito – Cyto)/Cyto. The cytoplasmic signal was first subtracted from the mitochondrial signal to remove any

signal that was contributed to the mitochondrial ROI from the cytoplasm above and below the mitochondria.

Cloning and Vector Information. All mammalian constructs were cloned into pLL 7.0 lentiviral vectors. Therefore, a CMV promoter drives expression. Mammalian constructs were assembled through PCR amplification and subsequent restriction enzyme digestion and ligation. The constructs were verified by sequencing. See Table S6 for more information and Addgene numbers.

Supplementary Figures

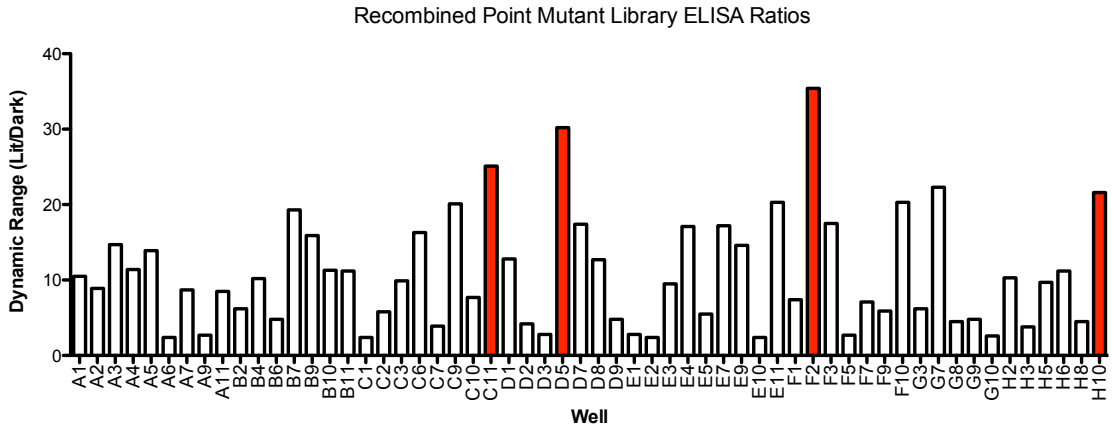

Fig. S1. ELISA recombined point mutant ratios. Lit/Dark signal ratios for top sequences out of recombined library. C11, D5, H10, and F2 were selected to characterize (red columns).

```
oLID        458 TDRATVRKIRDAIDNQTEVTVQLINYTKSGKKFWNLFHLQPMRDQK
C11         458 TDPATVRKIRDAIDNQTEVTVQLINYTKSGKKFWNMFHLQPMRDYK
D5          458 TDPATVRKIRDAIDNQTEVTVQLINYTKSGKKFWNVFHLQPMRDYK
H10         458 TDRATVRKIRDAIDNQTEVTVQLINYTKSGKKFWNMFHLQPMRDYK
F2 (iLID)   458 TDRATVRKIRDAIDNQTEVTVQLINYTKSGKKFWNVFHLQPMRDYK
                ** ********************************.********▲*

oLID        504 GDVQYFIGVQLDGTEHVRDAAEREAVMLIKKTAEEIDEAANDENYF
C11         504 GDVQYFIGVQLDGTERRRGAGEREAVILIKKTAFEIAEAANDENYF
D5          504 GDVQYFIGVQLDGTERLRGASEREAVILIKKTAFEIAEAANDENYF
H10         504 GDVQYFIGVQLDGTERRRGAGEREAVILIKKTAFEIAEAANDENYF
F2 (iLID)   504 GDVQYFIGVQLDGTERLHGAAEREAVCLIKKTAFQIAEAANDENYF
                ***************▲ .▲* ***** ******▲ *▲*********
```

Fig. S2. Sequence alignment of top four sequences. Residues left unmutated are shown in black (*), mutations having similar character to original amino acid are shown in grey (•), all other mutations are shown in white. Positions that converged to a single mutation in all 4 sequences have been marked with a red triangle (▲).

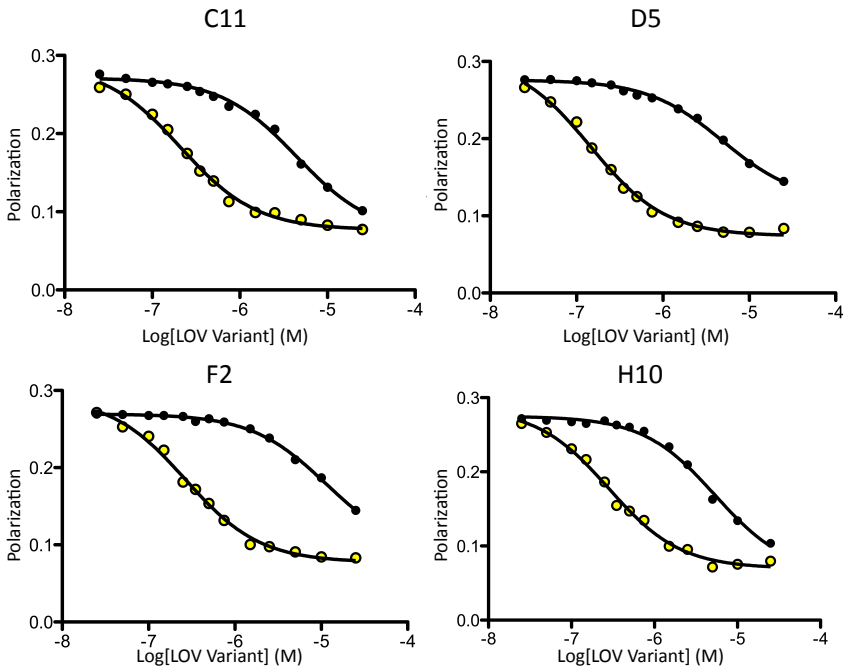

Fig. S3. *In vitro* binding data for top four sequences. Florescence polarization competition binding assays for the top four sequences (shown in Fig. S2). All four have a greater fold change in affinity than their parent oLID (Fig. 2B). Binding affinities can be found in Table S3.

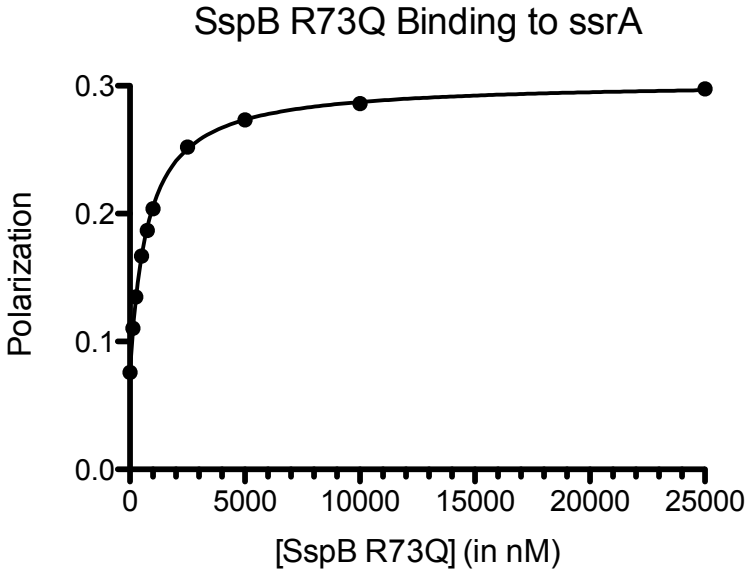

Fig. S4. Binding of SspB R73Q to ssrA peptide. Fluorescence polarization binding of ssrA labeled peptide to SspB R73Q (Micro). Affinity was measured to be 900 nM ± 200 nM.

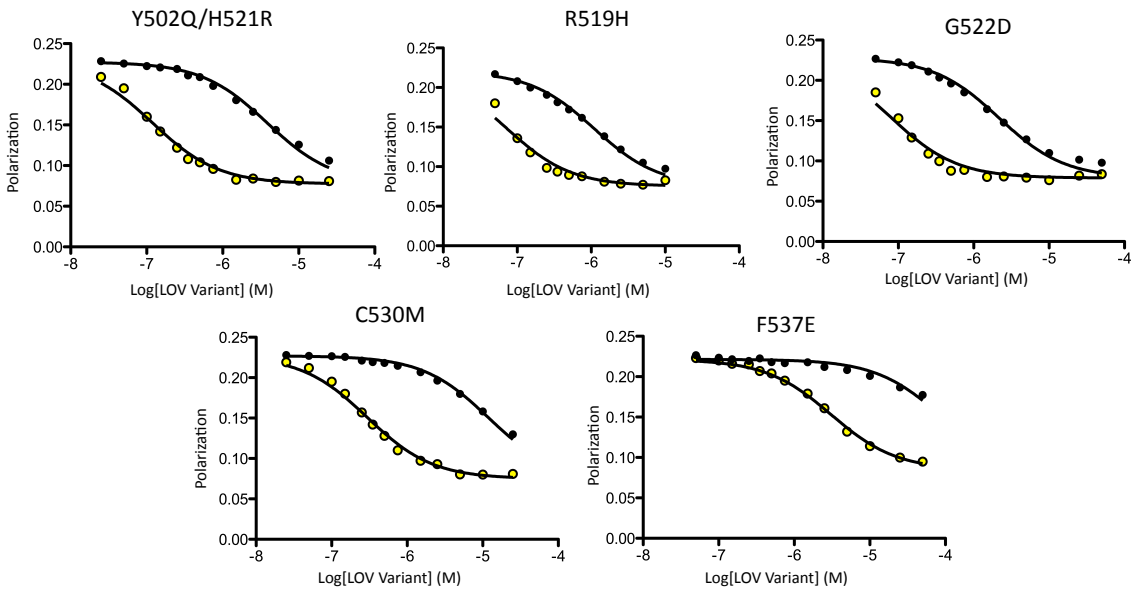

Fig. S5. *In Vitro* Binding of Reverted iLID Mutants. Florescence polarization competition binding assays for point mutation reversions show that only C530 can be removed without substantially affecting dynamic range or affinity range. Binding affinities can be found in Table S2.

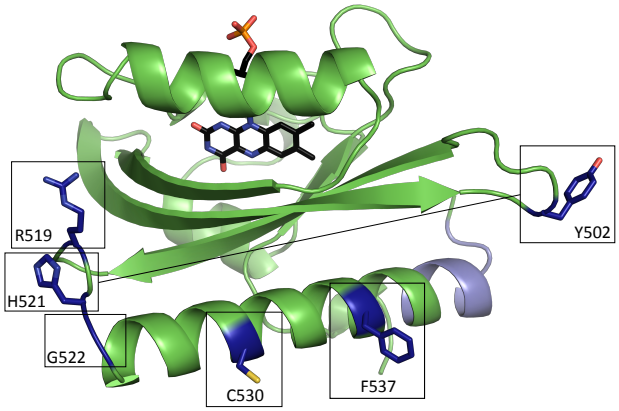

Mutation	Lit Affinity	Dark Affinity	Fold Change
iLID	132 ± 5 nM	4.7 ± 0.7 µM	36
Y502Q/ H521R	43 ± 1 nM	1.6 ± 0.1 µM	37
R519H	23 ± 1 nM	474 ± 1 nM	21
G522D	32 ± 1 nM	885 ± 1 nM	28
C530M	112 ± 1 nM	4.6 ± 0.1 µM	41
F537E	1.4 ± 0.1 µM	37.9 ± 0.3 µM	27

Fig. S6. Affinities of Reverted iLID Mutations. Reversion of iLID mutations elucidate role each plays in switch improvement. Left: structure of iLID with six mutations shown (boxes, dark blue). Right: Blue light and dark binding affinities due to the reversion of each of the mutations shown on left. C530 appears to have little to no effect on overall switching or range of affinity.

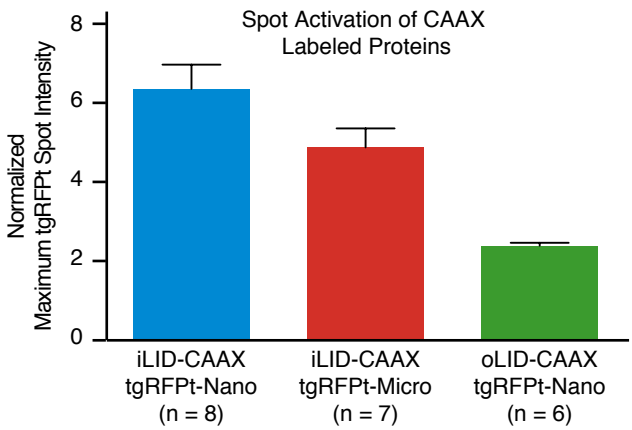

Fig. S7. The maximum recruitment of sspB to activated LIDs in cells. Measurements were made from a time course of localized activation as shown in Fig. 4A, Row 2. The maximum tgRFPt signal intensity in an activated region of a cell, normalized to the intensity before activation was measured.

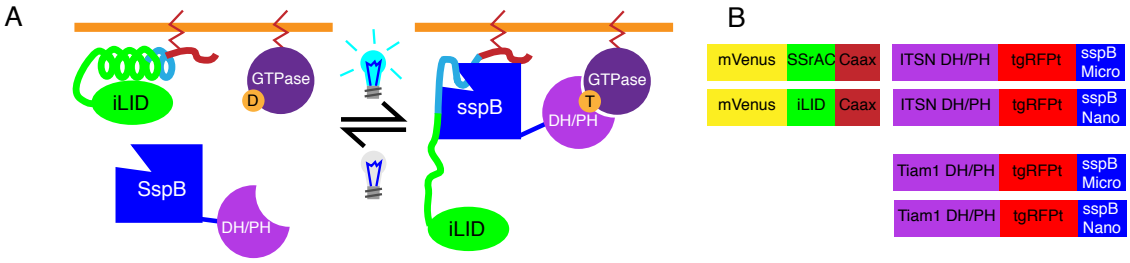

Fig. S8. Activating GTPase pathways through GEF recruitment. (*A*) A schematic, demonstrating that in the absence of blue light, Micro fused to a DH/PH domain remains cytoplasmic and inactive. In the presence of blue light, Micro fused to the DH/PH domain binds to iLID, localizing the DH/PH to the membrane, where it increases the rate of GTPase nucleotide exchange to induce signaling. (*B*) Schematic of constructs made and tested.

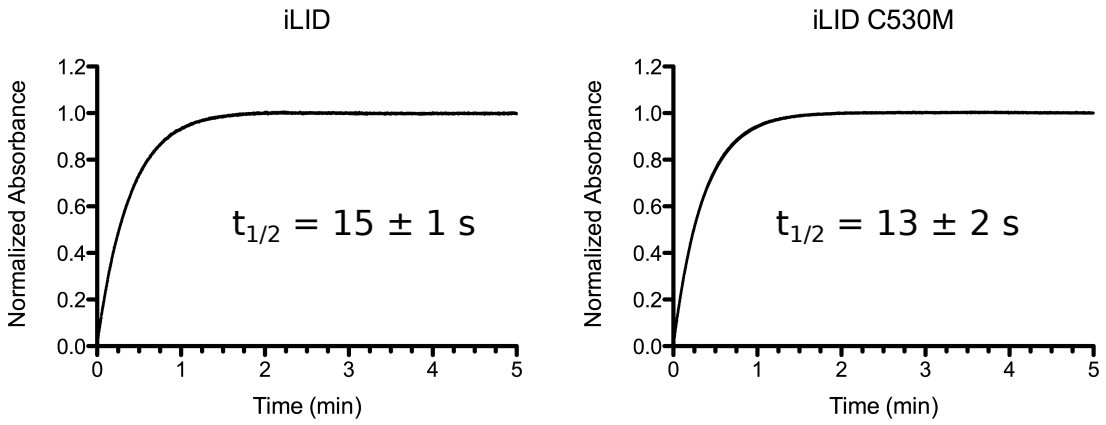

Fig. S9. Thermal Reversion of iLID and iLID C530M. Reversion of iLID C530M (right) yields similar reversion kinetics as iLID (left). Experiments were performed at room temperature.

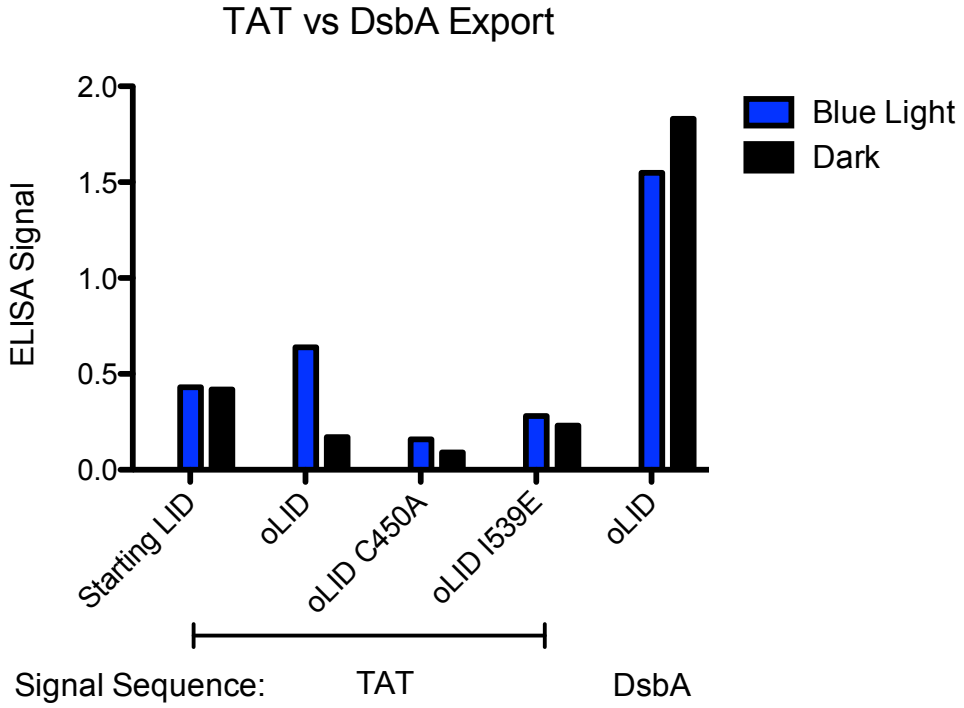

Fig. S10. Binding of LIDs expressed via Tat and SRP pathways to SspB. Secretion of LID constructs via the TAT pathway yields functional protein that binds immobilized SspB in a light-dependent fashion. Using the DsbA signal sequence, the secreted protein does not bind SspB tighter under blue light than in darkness.

Video S1. Video corresponding to images in Fig. 4A Top Row.

Video S2. Video corresponding to images in Fig. 4A Bottom Row.

Video S3. Video corresponding to images in Fig. 4C.

Video S4. Video corresponding to images in Fig. 5A.

Video S5. Video corresponding to images in Fig. 5B.

Video S6. Localized ITSN leads to dramatic increase in endocytosis. Fibroblast expressing Venus-iLID-caax (green) and ITSN-tgRFPt-Nano (Red). The cell was photostimulated in the marked ROIs, producing a large protrusion as well as an exaggerated increase in endocytosis at the ROI. The fluorescence intensities were adjusted in both channels the make the DIC image (Grey) more clear.

Table S1. Beginning and Improved iLID affinities

Construct	**Blue Light Affinity**	**Dark Affinity**
Starting LOV-SsrA	0.031 ± 0.006 μM*	0.057 ± 0.005 μM*
LOV-SsrAC	0.120 ± 0.01 μM*	0.9 ± 0.07 μM*
iLID nano	0.132 ± 0.005 μM	4.7 ± 0.7 μM
iLID micro	0.8 ± 0.1 μM	47 ± 13 μM
SspB R73Q	-	0.9 ± 0.2 μM

*Previously published values

Table S2. Reversion Mutation Affinities

Construct	**Blue Light Affinity**	**Dark Affinity**	**Fold Change**
iLID nano	0.132 ± 0.005 μM	4.7 ± 0.7 μM	36
502/521	0.043 ± 0.005 μM	1.60 ± 0.05 μM	37
519	0.024 ± 0.004 μM	0.49 ± 0.05 μM	20
522	0.032 ± 0.01 μM	0.88 ± 0.04 μM	28
530	0.113 ± 0.004 μM	4.6 ± 0.6 μM	41
537	1.4 ± 0.1 μM	37.3 ± 0.7 μM	27

Table S3. Top ELISA Sequence Affinities

Construct	**Blue Light Affinity**	**Dark Affinity**
D5	77 ± 0.001 μM*	3.4 ± 0.02 μM*
C11	97 ± 0.001 μM*	1.7 ± 0.03μM*
H10	123 ± 0.001 μM*	2.0 ± 0.02 μM*
F2 (iLID nano)	0.132 ± 0.005 μM	4.7 ± 0.7 μM

*Error shown is standard error to binding curve fit

Table S4. Rosetta predicted point mutations included in library

Residue #	Mutations	WT AA	Rosetta Predicted Library
404	13	L	ACDEGKMNQRSTY
406	1	T	S
407	17	T	ACDEFGIKLMNPQRSVY
408	3	L	MTV
411	5	I	KLQRV
413	11	K	ACDEHMNQRSW
414	3	N	AHS
415	1	F	H
417	4	I	VTLA
428	14	I	ACEGHKLMNQRSTV
429	4	F	HKRY
431	1	S	A
475	9	E	ACKMQRSTV
477	3	T	CAV
479	2	Q	EI
493	13	L	ACDEGHIMNQSTV
497	6	Q	AEHKMR
499	14	M	ACDEFHKNQRSTWY
500	9	R	ACEIKMQTV
502	15	Q	ACDEGHIKLMNRSTV
508	7	Y	ACFHKMR
510	4	I	VTLC
512	1	V	T
514	3	L	MQY
519	16	H	ACDEFIKMNPQRSVWY
520	13	V	ACDFHKLMNRSTY
521	13	R	ACEGHKMNQSTVY
522	15	D	ACEFGHKLMNQRSWY
523	15	A	CDEGIKLMNQRSTVY
524	11	A	CDEGKLMNQRS
525	10	E	AFHKLMQRWY
526	17	R	ACDEFGIKLMNQSTVWY
527	16	E	ACDGIKLMNQRSTVWY
529	15	V	ACDEFHIKMNQRTWY
530	18	M	ACDEFGHIKLNQRSTVWY
531	18	L	ACDEFGHIKMNQRSTVWY
532	5	I	AMSTV
533	10	K	AEHLMQRTVY
534	17	K	ACDEFGILMNQRSTVWY
535	18	T	ACDEFGHIKLMNQRSVWY
537	12	E	ACDIKLMNQRTV
539	3	I	LTV
540	16	D	ACEFGHKLMNQRSTWY
541	14	E	ACDIKLMNQRSTVY

Table S5. Data collection and refinement statistics

Wavelength (Å)	1.0
Resolution range (Å)	31.08 - 1.95 (2.02 - 1.95)
Space group	P 21 21 21
Unit cell	62.156 70.339 80.378 90 90 90
Total reflections	158984
Unique reflections	26276 (2574)
Multiplicity	6.0
Completeness (%)	99.8 (100.00)
Mean I/sigma(I)	9.63 (2.41)
Wilson B-factor	25.4
R-merge	0.088
R-meas	0.038
R-work	0.231 (0.356)
R-free	0.244 (0.398)
Number of non-hydrogen atoms	2711
Macromolecules	2392
Ligands	63
Water	256
Protein residues	288
RMS(bonds)	0.013
RMS(angles)	1.26
Ramachandran favored (%)	99
Ramachandran outliers (%)	0
Clashscore	6.36
Average B-factor	29.5
Macromolecules	28.4
Ligands	30.6
Solvent	39.8

Statistics for the highest-resolution shell are shown in parentheses.

Table S6. Construct Information

Construct	Description	Addgene ID
***E. coli* Expression**		
iLID	pQE-80L: iLID (C530M)	60408
SspB Nano	pQE-80L: MBP-SspB WT	60409
SspB Micro	pQE-80L: MBP-SspB R73Q	60410
Mammalian Cell		
Venus-iLID-CAAX	pLL7.0: Venus-iLID-CAAX (from KRas4B)	60411
Venus-oLID-CAAX	pLL7.0: Venus-oLID-CAAX (from KRas4B)	60412
Venus-iLID-Mito	pLL7.0: Venus-iLID-Mito (From ActA)	60413
Venus-oLID-Mito	pLL7.0: Venus-iLID-Mito (From ActA)	60414
tgRFPt-Nano	pLL7.0: tgRFPt-SSPB WT	60415
tgRFPt-Micro	pLL7.0: tgRFPt-SSPB R73Q	60416
Tiam DH/PH-tgRFPt-Nano	pLL7.0: mTiam1(64-437)-tgRFPt-SSPB WT	60417
Tiam DH/PH-tgRFPt-Micro	pLL7.0: mTiam1(64-437)-tgRFPt-SSPB R73Q	60418
ITSN DH/PH-tgRFPt-Nano	pLL7.0: hITSN1(1159-1509)-tgRFPt-SSPB WT	60419
ITSN DH/PH-tgRFPt-Micro	pLL7.0: hITSN1(1159-1509)-tgRFPt-SSPB R73Q	60420

References

1. Firnberg E, Ostermeier M (2012) PFunkel: Efficient, Expansive, User-Defined Mutagenesis. *PLoS One* 7.

2. Tonikian R, Zhang Y, Boone C, Sidhu SS (2007) Identifying specificity profiles for peptide recognition modules from phage-displayed peptide libraries. *Nat Protoc* 2:1368–86. Available at: http://www.ncbi.nlm.nih.gov/pubmed/17545975 [Accessed September 11, 2014].

3. Kabsch W (2010) XDS. *Acta Crystallogr Sect D Biol Crystallogr* 66:125–132.

4. Winn MD et al. (2011) Overview of the CCP4 suite and current developments. *Acta Crystallogr Sect D Biol Crystallogr* 67:235–242.

5. Evans P (2006) in *Acta Crystallographica Section D: Biological Crystallography*, pp 72–82.

6. McCoy AJ et al. (2007) Phaser crystallographic software. *J Appl Crystallogr* 40:658–674.

7. Adams PD et al. (2010) PHENIX: A comprehensive Python-based system for macromolecular structure solution. *Acta Crystallogr Sect D Biol Crystallogr* 66:213–221.

8. Emsley P, Lohkamp B, Scott WG, Cowtan K (2010) Features and development of Coot. *Acta Crystallogr Sect D Biol Crystallogr* 66:486–501.

9. Schindelin J et al. (2012) Fiji: an open-source platform for biological-image analysis. *Nat Methods* 9:676–682.